RSC Advances

PAPER

View Article Online
View Journal | View Issue

Cite this: *RSC Adv.*, 2021, **11**, 38316

Phase behavior and interfacial tension of ternary polymer mixtures with block copolymers†

Dongmei Liu,[a] Ye Lin,[a] Kai Gong,[a] Huifeng Bo,*[a] Deyang Li,[a] Zhanxin Zhang[a] and Wenduo Chen*[b]

Received 17th October 2021
Accepted 22nd November 2021

DOI: 10.1039/d1ra07671j

rsc.li/rsc-advances

The phase behavior and interfacial tension of ternary polymeric mixtures (polystyrene/polystyrene-*b*-poly(methyl methacrylate)/poly(methyl methacrylate), PS/PS-*b*-PMMA/PMMA) are investigated by dissipative particle dynamics (DPD) simulations. Our simulation results show that, as the PS-*b*-PMMA diblock copolymer concentration increases, the interfacial tension decreases due to the decayed correlations between homopolymers PS and PMMA. When the chain lengths of copolymers are fixed, with the increase of the chain lengths of PS and PMMA homopolymers the interfacial width becomes wider and the interfacial tension becomes smaller, due to the copolymers presenting more stretched and swollen structures in the mixtures with the short length of homopolymers. However, with simultaneously increasing chain lengths of both diblock copolymer and homopolymers with a fixed ratio, the interfacial tension increases because the copolymer chains with longer chain length penetrate more deeply into the homopolymer phase and the interactions between diblock copolymers become weaker. These results will provide a way to mix incompatible homopolymers to improve material performances.

1. Introduction

In recent years, polymeric mixtures composed of block copolymers and homopolymers have become one of the most popular research issues in the field of polymer science and engineering.[1–4] It is known that chemically different polymers are usually immiscible,[5] which inhibits the increase in mixing entropy[6] and forms a thin interface with larger interfacial tension. The formation of thermodynamically stable polymeric mixtures is generally caused by the substantial decrease of the interfacial tension by the addition of copolymer compatibilizers between incompatible homopolymers, which results in the improved performance of the polymer composite materials.[7] The copolymer compatibilizers at the interface could change the aggregation states of the immiscible homopolymers to minimize the interfacial energy. Thus, it is important to investigate the interfacial tension and structure of phase-separated polymeric mixtures at the molecular level.

Experimental studies of the ternary homopolymer/block copolymer (homopolymer/block copolymer/homopolymer) mixtures have been extensively performed. By using neutron reflectivity and elastic recoil detection, Russell *et al.*[8–12] investigated the density distribution of symmetric PS-*b*-PMMA chains, the width between the PS and PMMA homopolymers, and the interfacial tension. They found that the interfacial width between the PS and PMMA homopolymers broadens with the addition of the PS-*b*-PMMA chains, which increases from 50 Å at the absence of the PS-*b*-PMMA chains up to ~85 Å at interfacial saturation. When the copolymer chains segregate to the interface, the interfacial tension decreases, which is consistent with the changing of interfacial tension in similar experimental works. Liu *et al.*[13] investigated the dependence of phase behavior and dimensional scaling for PS/PS-*b*-PMMA/PMMA ternary mixtures on the χN (χ and N represent the Flory–Huggins interaction parameter and the degree of polymerization of PS-*b*-PMMA chain, respectively), the α (the ratio of the degree of polymerization of the PS and PMMA chains to that of the PS-*b*-PMMA chains), and the volume fraction of homopolymers in the mixtures. They found that the phase of the mixtures depends weakly on χN and α, but as the volume fraction of homopolymers increases, the phase transitions from lamellae to microemulsion and then to macrophase-separated domains. Morse *et al.*[14] measured the interfacial tension between polystyrene and polybutadiene homopolymers in the presence of poly(styrene-*b*-butadiene) copolymer. The results showed that as the copolymer is premixed with PS, the interfacial tension presents a decrease with increasing concentration until an apparent CMC (critical micelles concentration) and then saturating at higher concentrations.

With the rapid development of computer hardware and software technology, molecular simulations have become a vital method for studying the phase morphology and mechanical

[a]*School of Science, North China University of Science and Technology, Tangshan 063210, P. R. China. E-mail: bohuifeng@ncst.edu.cn*

[b]*School of Materials, Sun Yat-sen University, Guangzhou 510275, P. R. China. E-mail: chenwd29@mail.sysu.edu.cn*

† Electronic supplementary information (ESI) available. See DOI: 10.1039/d1ra07671j

properties of polymeric mixtures. Fischel *et al.*[15] employed the self-consistent field method to investigate PS/PS-*b*-PMMA/PMMA mixtures. They found an excellent qualitative and quantitative agreement with the experimental data for the volume fraction profiles of both homopolymers and blocks of the copolymer at the interface. Balazs *et al.*[16–20] reported a series of Monte Carlo simulations for the ternary block copolymer/homopolymer mixtures. Doi *et al.*[21] derived the expression for the free energy of copolymer blends as a function of the density distribution of the monomer on each block. This expression can be used to calculate the micro- and macro-phase separation of any blends of homopolymers and block copolymers with arbitrary topological structures. Matsen *et al.*[22,23] and Fredrickson *et al.*[24–26] reported a series of field theoretic simulations to predict the equilibrium phase diagram of symmetric blends of AB diblock copolymer with A and B homopolymers. Their results are in qualitative agreement with the results of experiments in this system. Tanaka *et al.*[27] investigated the local orientation of PS segments of the PS-*b*-PMMA chains at the interface by atomistic molecular dynamics simulation. It is found that the PS-*b*-PMMA chains which are located on the interfacial region, are in-plane oriented. In recent years, dissipative particle dynamics (DPD) simulations have been successfully used to study the interfacial and structural properties of immiscible mixtures.[28–39] Specifically, Qian *et al.*[28] calculated the interfacial tension of homopolymer/diblock copolymer/homopolymer mixtures *via* DPD simulation, and the results show that, as the number of the AB copolymer is fixed, the interfacial tension decreases with the increase of chain length of AB copolymer. Guo *et al.*[29] systematically investigated the segregation of block copolymers in binary immiscible homopolymer blends through DPD simulations. They found that swollen block copolymers are more efficient in reducing the interfacial tension than nonswollen block copolymers. Pinto *et al.*[30] investigated the effects of copolymer structure and concentration on the homopolymer/copolymer/homopolymer mixtures by DPD simulation. They proved that the microstructural properties of the copolymer exert a decisive impact on molecular interactions and the characteristics of the mesophases generated during the blending process. Goodson *et al.*[31] performed a DPD simulation to study the effect of the interaction parameters of beads, chain length, and content of homopolymers on morphological stability and phase diagram of symmetric ternary mixtures PS/PS-*b*-PMMA/PMMA, which reproduce the key features of the experiment.

The above studies have increased our understanding of interfacial properties for homopolymer/block copolymer/homopolymer mixtures, whereas there are still many questions remaining unclear. In this research, we employ the DPD method to systematically explore the phase behavior and interfacial tension of the ternary polymeric mixtures PS/PS-*b*-PMMA/PMMA (S_n/$S_m$$M_m$/$M_n$). The methods are constructed based on Goodson's[31] and our previous works.[40–44] The dependence of the interfacial tension, the interfacial width, and the detailed chain conformations on the copolymer concentration, the chain lengths of homopolymers, and the simultaneous change of chain length of PS-*b*-PMMA, PS, and PMMA are systematically examined. The result elucidates that the more addition of the PS-*b*-PMMA copolymers, the shorter the PS-*b*-PMMA, PS, PMMA chain lengths, the lower the interfacial tension when the ternary mixtures occur macrophase segregation. Finally, the summary of our results and some concluding remarks are given in conclusions.

2. Model and simulation

2.1 Model

Dissipative particle dynamics is developed to study mesoscale problems in complex fluids and soft matter,[45] which has the following two important features, compared with traditional all-atom molecular dynamics. First, a coarse-grained bead generally represents tens of monomer units in a DPD simulation system, which means that a larger time and a longer length scale can be achieved. Second, the beads in the system can overlap in a large amount, since the interactions between the paired beads occur through a soft potential.[30]

DPD method can be used to study highly dispersed polymer mixtures without significant influence on mathematical formulas and calculation procedures, which is another special advantage. In a DPD simulation, all beads follow Newton's equations of motion,

$$\frac{\mathrm{d}\mathbf{r}_i}{\mathrm{d}t} = \mathbf{v}_i; \quad m_i \frac{\mathrm{d}\mathbf{v}_i}{\mathrm{d}t} = \mathbf{f}_i \tag{1}$$

where vector $\mathbf{r}_i$ and $\mathbf{v}_i$ denote the position and velocity of the bead marked as i in the system, respectively. The mass m_i is assumed to be 1 in the reduced unit. The total force $\mathbf{f}_i$ acting on ith bead can be written as the sum of the conservative force $\mathbf{F}_{ij}^{\mathrm{C}}$, drag force $\mathbf{F}_{ij}^{\mathrm{D}}$, random forces $\mathbf{F}_{ij}^{\mathrm{R}}$ and the spring force $\mathbf{F}_i^{\mathrm{S}}$:[32]

$$\mathbf{f}_i = \sum_{i \neq j} \left(\mathbf{F}_{ij}^{\mathrm{C}} + \mathbf{F}_{ij}^{\mathrm{D}} + \mathbf{F}_{ij}^{\mathrm{R}} \right) + \mathbf{F}_i^{\mathrm{S}} \tag{2}$$

The conservative force $\mathbf{F}_{ij}^{\mathrm{C}}$, represented by a soft potential, which is generally expressed as[32]

$$\mathbf{F}_{ij}^{\mathrm{C}} = \begin{cases} -\alpha_{\mathrm{SM}}(1 - r_{ij})\mathbf{e}_{ij} & (r_{ij} < 1) \\ 0 & (r_{ij} \geq 1) \end{cases} \tag{3}$$

where α_{SM} is repulsion force parameter, which is a constant greater than 0, hence $\mathbf{F}_{ij}^{\mathrm{C}}$ is always repulsive. The distance between ith bead and jth bead is represented by r_{ij}, and is equal to the absolute value of the vector $\mathbf{r}_{ij} = \mathbf{r}_i - \mathbf{r}_j$, *i.e.*, $r_{ij} = |\mathbf{r}_{ij}|$. $\mathbf{e}_{ij} = \mathbf{r}_{ij}/r_{ij}$ is the unit vector, which is in the same direction with $\mathbf{r}_{ij}$.[32]

The dissipative force $\mathbf{F}_{ij}^{\mathrm{D}}$ depicts viscous drag and the random force $\mathbf{F}_{ij}^{\mathrm{R}}$ signifies the stochastic impulse, usually are given as follows:

$$\mathbf{F}_{ij}^{\mathrm{D}} = -\gamma\omega^{\mathrm{D}}(r_{ij})(\mathbf{v}_{ij} \cdot \mathbf{e}_{ij})\mathbf{e}_{ij} \tag{4}$$

$$\mathbf{F}_{ij}^{\mathrm{R}} = \sigma\omega^{\mathrm{R}}(r_{ij})\xi_{ij}\Delta t^{-1/2}\mathbf{e}_{ij} \tag{5}$$

in which $\mathbf{v}_{ij} = \mathbf{v}_i - \mathbf{v}_j$. The parameter γ is the friction coefficient which signifies the dissipation strength. σ is the amplitude of

the noise, and ξ_{ij} is the Gaussian fluctuating variable with zero mean value. ω^{D} and ω^{R} are dimensionless weighting functions of the dissipative forces $\mathbf{F}_{ij}^{D}$ and random forces $\mathbf{F}_{ij}^{R}$, respectively. They satisfy the fluctuation-dissipation theorem[32]

$$\omega^{D}(r) = [\omega^{R}(r)]^2,\ \sigma^2 = 2\gamma k_B T \tag{6}$$

where k_B is the Boltzmann constant and T is the thermodynamics temperature.

The dimensionless weighting functions $\omega^{R}(r_{ij})$ and $\omega^{R}(r_{ij})$ can be simply taken from the research of Groot and Warren,[32]

$$\omega^{D}(r) = \left[\omega^{R}(r)\right]^2 = \begin{cases} (1-r)^2 & (r<1) \\ 0 & (r\geq 1) \end{cases} \tag{7}$$

The harmonic spring force between the bonded beads enforces bead connectivity and is expressed as

$$\mathbf{F}_i^{S} = \sum_{j\neq i} C\mathbf{r}_{ij} \tag{8}$$

where the spring force constant $C = 4.0$.

The repulsion interaction parameter α_{SM} can be mapped to the Flory–Huggins parameter χ_{SM} *via* the following correlation[32]

$$\alpha_{SM} \approx \alpha_{SS} + 3.50\chi_{SM} \tag{9}$$

where α_{SS} and α_{SM} are the repulsion parameter of identical and different kinds of beads, respectively. The Flory–Huggins interaction parameter is taken from the work of Albert *et al.*[31] *i.e.*, $\alpha_{SS} = \alpha_{MM} = 25$ and $\alpha_{SM} = 65$, which could reproduce the experimental behavior for PS-*b*-PMMA blended with PS and PMMA.[13] Compared this parameter to the Flory–Huggins interaction parameter 0.032 [macromolecules 1993, 26, 5819], one DPD bead represents tens of monomers.

2.2 Simulation details

In this work, the DPD simulations are operated in a periodic cubic box with a side length $L = 30$ by Materials Studio (Accelrys Inc.) software. For simplicity, the radius of interaction is taken as $r_c = 1$ and the temperature $k_B T = 1$. The simulated bead density $\rho = 3$.[28] The friction coefficient $\gamma = 4.5$. In this simulation, the program is first performed 2.0×10^5 steps to ensure that the system has reached equilibration with the time steps 0.05 (in reduced units). Then, the program is performed 5×10^4 steps as the production runs. We calculate the square of the radius of gyration of copolymers to show that the equilibration and production phase are sufficiently long (as illustrated in Fig. S1 in the ESI†), the evolution of the blend's morphology also show that the systems have reached equilibration [Fig. S2†]. To ensure the accuracy of the results, we ran 5 parallel simulations and averaged.

In all cases, the $S_n/S_mM_m/M_n$ mixtures contain equal amounts of PS, PMMA homopolymers, and the chain length of the homopolymers PS and PMMA are equal, the PS-*b*-PMMA diblock also consists of the same number of S and M beads.

To characterize the structure of PS/PS-*b*-PMMA/PMMA mixtures, we calculated the static structure factor, which obeys the following relationship,

$$S_{SS}(q) = \frac{1}{m}\sum_{i=1}^{m}\sum_{j=1}^{m}\left\langle e^{-i\mathbf{q}\cdot(\mathbf{r}_i-\mathbf{r}_j)}\right\rangle \tag{10}$$

where q represents the wave vector,[30] $\mathbf{r}_i$ and $\mathbf{r}_j$ are the position vectors of ith and jth S beads in S_mM_m copolymer chains, m is the number of beads S in S_mM_m chains. By analyzing the static factor, we can identify different phases and determine the transitions due to the increase of copolymer concentration. It is noted that there are only certain q-values can be included in our system, due to the periodic boundary conditions.

The interfacial tension is one of the most important parameters which can directly reflect the mechanical properties and stability of the interface in the phase-separated mixtures with a flat interface. Here, the interfacial tension was calculated by the following formula,[46]

$$\gamma_{DPD} = \frac{1}{2}\int\left[P_{xx} - \frac{1}{2}\left(P_{yy}+P_{zz}\right)\right]dx \tag{11}$$

where P_{xx} is the pressure tensor normal to the interface, P_{yy} and P_{zz} are the pressure tensor parallel to the interfaces.

To characterize the detailed conformations of the PS-*b*-PMMA chain, the mean-square radii of gyration $\langle R_g^2\rangle$, the mean-square end-to-end distance $\langle R_{ee}^2\rangle$, and the chain orientation parameter Θ were also calculated. The orientation parameter Θ of the PS-*b*-PMMA chain is calculated by the equation,[28]

$$\Theta = \frac{\left(\langle R_g^2\rangle_x - 1/2\left(\langle R_g^2\rangle_y + \langle R_g^2\rangle_z\right)\right)}{\langle R_g^2\rangle} \tag{12}$$

where $\langle R_g^2\rangle_x$, $\langle R_g^2\rangle_y$, $\langle R_g^2\rangle_z$ are the normal and transverse components of the mean-square radii of gyration $\langle R_g^2\rangle$, respectively.

In addition, the interfacial width w between the PS and PMMA homopolymers was calculated by fitting the function $\tanh((x+d)/w)$ to the profile $(\rho^A(x) - \rho^B(x))/\rho(x)$ across the two interfaces, where d is the position of the interface center in x-directions.[29]

3. Results and discussion

3.1 Morphology and structures of $S_n/S_mM_m/M_n$ ternary mixtures

To investigate how the diblock copolymer concentration c_{cp} (c_{cp} is referred as the number density of the copolymer) influences the phase behavior and structural properties of the mixtures, we vary the PS-*b*-PMMA chains concentration from $c_{cp} = 0.0$ to $c_{cp} = 1.0$ for $S_2/S_5M_5/M_2$ mixtures. Fig. 1 and 2 show the representative morphology snapshots and structure-factor $S_{SS}(q)$ for $S_2/S_5M_5/M_2$ mixtures at different S_5M_5 copolymer concentrations c_{cp}, respectively.

It is clear that the mixtures of homopolymers S_2 and M_2 show phase separation in the absence of S_5M_5 copolymers Fig. 1(a). When the content of the S_5M_5 chains increases from $c_{cp} = 0.01$ to 0.2, two flat interfaces formed between the S_2 and M_2

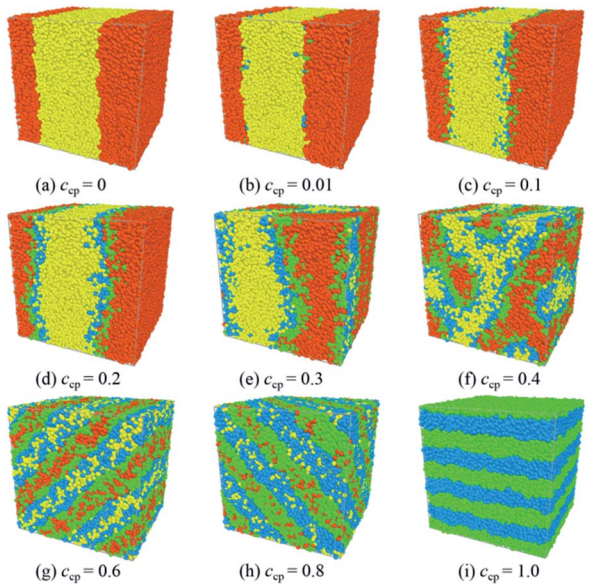

Fig. 1 (a)–(i) Morphology snapshots for $S_2/S_5M_5/M_2$ mixtures at different S_5M_5 diblock copolymer concentration c_{cp}. The red and yellow spheres denote bead S and bead M of homopolymers PS and PMMA, and the green and blue spheres represent beads S and M of the diblock PS-*b*-PMMA, respectively.

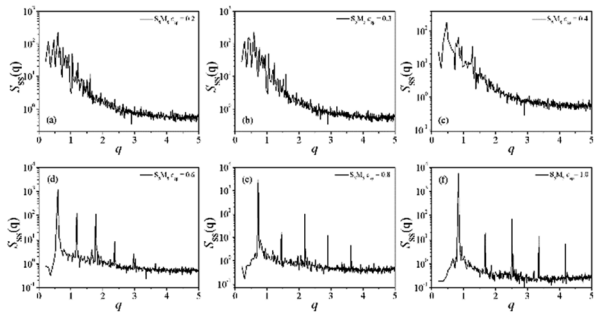

Fig. 2 Structure-factor $S_{SS}(q)$ of the S beads in copolymer with S_5M_5 concentration of (a) $c_{cp} = 0.2$ (b) $c_{cp} = 0.3$ (c) $c_{cp} = 0.4$ (d) $c_{cp} = 0.6$ (e) $c_{cp} = 0.8$ (f) $c_{cp} = 1.0$.

homopolymers, which populated with the S_5M_5 copolymers. The S beads of the S_5M_5 copolymers penetrate into the S_2 homopolymer phase, and the M beads penetrate into the M_2 homopolymer phase Fig. 1(b)–(d). This phenomenon verifies the simulation results by Albert *et al.*[31]

As the S_5M_5 chains concentration increases from $c_{cp} = 0.2$ to $c_{cp} = 0.3$, the interfacial geometry starts to change and no longer remains a flat shape Fig. 1(e). However, as shown in Fig. 2, the structure factor $S_{SS}(q)$ in this concentration still displays its maximum at the smallest value of q, which indicates that the mixtures remain in a state of macrophase segregation.[30,47]

When the S_5M_5 diblock concentration is $c_{cp} = 0.4$, several peaks appear in the structure factor $S_{SS}(q)$, indicating that the mixtures have formed a bicontinuous structure Fig. 1(f) and 2(c). When $c_{cp} \geq 0.6$, the mixtures form lamellar structures Fig. 1(g)–(i). The S_2 homopolymers disperse in the S beads in S_5M_5 diblock copolymers. The scattering intensity displays five peaks Fig. 2(d), with the thickness of lamellae is $2\pi/q > 10.5$. When $c_{cp} = 1.0$, the thickness of lamellae decreases to around 7, which indicates that as the S_5M_5 diblock concentration increases, the width of the lamellar domains decreases.

We have verified that the S_5M_5 diblock copolymers are segregated at the interfaces between the S_2 and M_2 homopolymers phase when $c_{cp} \leq 0.2$. According to the experimental research of Russell *et al.*,[8–12] when the S_mM_m chains aggregate at the interfaces, they can significantly change the density distribution of the S_n and M_n homopolymers and then affect the interfacial tension. Therefore, in the next part of the manuscript, we investigate the effect of increasing the S_5M_5 chains concentration c_{cp} on the interfacial tension, *etc.*, interfacial properties. We define the direction of perpendicular to the interfaces is *x*-direction in the lamellar structures.

3.2 Interfacial tension for $S_n/S_mM_m/M_n$ mixtures

Fig. 3(a) and (b) show the density profiles (ρ) of beads S and M of S_5M_5 chains and S_2, M_2 homopolymers as a function of c_{cp}. As the concentration of S_5M_5 chains increases from $c_{cp} = 0.01$ to $c_{cp} = 0.2$, the densities of the beads S and M of S_5M_5 chains at the interfaces exhibit significant increases Fig. 3(a), while the densities of the beads S and M of homopolymers S_2 and M_2 at the interface decreases Fig. 3(b). It can be understood that the accumulation of S_5M_5 diblock copolymers at the interface pushes the S_2 and M_2 homopolymers further away from the interfaces. This result also illustrates the decayed correlations between homopolymers S_2 and M_2 with increasing the S_5M_5 chain concentration c_{cp}.

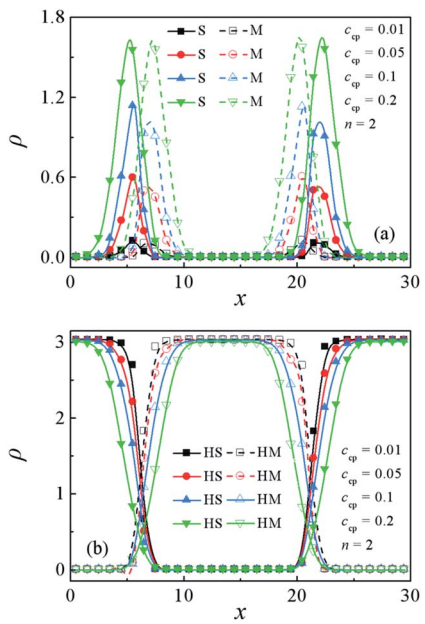

Fig. 3 Density profiles of beads S and M of (a) S_5M_5 copolymers and (b) S_2 and M_2 homopolymers in the *x*-direction as a function of the concentration of the S_5M_5 chains.

In order to quantify the effect of increasing the S_mM_m chains concentration c_{cp} on the interfacial properties for the $S_n/S_mM_m/M_n$ mixtures. The interfacial tension γ and interfacial width w at different S_5M_5 chains concentrations c_{cp} with $n = 2$ and $n = 10$ are calculated, as shown in Fig. 4(a) and (b). Apparently, the interfacial tension γ decreases while the interfacial width w increases between the S_n and M_n homopolymers with increasing the S_5M_5 concentration c_{cp} in the mixture systems. We infer that the decrease of the interfacial tension γ and the increase of the interfacial width w are related to the density distribution of the S_5M_5 copolymers and S_n, M_n homopolymers as illustrated in Fig. 3(a) and (b). That is, as the S_5M_5 diblock copolymer concentration c_{cp} increases from 0.01 to 0.2, the densities of the S, M beads of S_5M_5 diblock at the interfaces exhibit a significant increase, while the densities of the homopolymers S_n, M_n near the center of the interfaces decrease, which results in the decayed correlations between S_n and M_n homopolymers. Hence, the interfacial tension γ decreases, the interfacial width w increases. We also find that the interfacial tension γ has a smaller value for shorter homopolymer chain length $n = 2$ at the fixed S_5M_5 diblock concentration, which implies that the S_5M_5 diblock shows better performance in lowering the interfacial tension γ for the mixtures with the shorter S_2 and M_2 homopolymer. These results for the interfaces are in good agreement with the previous studies.[29]

Moreover, to characterize the configurations of the S_5M_5 chains, we calculate the chain orientation parameter Θ, mean-square radii of gyration $\langle R_g^2 \rangle$ and its three components $\langle R_g^2 \rangle_x$, $\langle R_g^2 \rangle_y$, $\langle R_g^2 \rangle_z$ of the S_5M_5 diblock copolymer. Fig. 4(c) and 5 depict the dependence of the chain orientation parameter Θ and the dimension of the S_5M_5 diblock copolymers on the copolymer concentration c_{cp}. We found that the S_5M_5 chain orientation parameter Θ is greater than 0, and increases with increasing c_{cp} Fig. 4(c), which indicates that the S_5M_5 diblock copolymer with higher concentration is more stretched in the x-direction (perpendicular to the interface). Fig. 5 shows that the S_5M_5 copolymers exhibit almost the same sizes in y and z directions, which are parallel to the interfaces, and both y and z components are smaller than the perpendicular x component see Fig. 5(a) and (b). The $\langle R_g^2 \rangle$ and $\langle R_g^2 \rangle_x$ increase with increasing the S_5M_5 diblock copolymer concentration c_{cp} as illustrated in Fig. 5(a) and (b). This result also indicates that increasing the S_5M_5 diblock copolymer concentration c_{cp} causes the S_5M_5 diblock copolymer to extend along the x-direction.

As shown by Fig. 4 and 5, the chain length of PS and PMMA homopolymers exhibit a significant effect on the interfacial properties of the $S_n/S_mM_m/M_n$ ternary mixtures. Therefore, in the following part of the manuscript, we explored the effects of increasing the homopolymer chain length n (the S_mM_m chain length is fixed as 10) and the simultaneous change of chain lengths of S_mM_m, S_n, M_n chain lengths ($m = n$) on the interfacial properties.

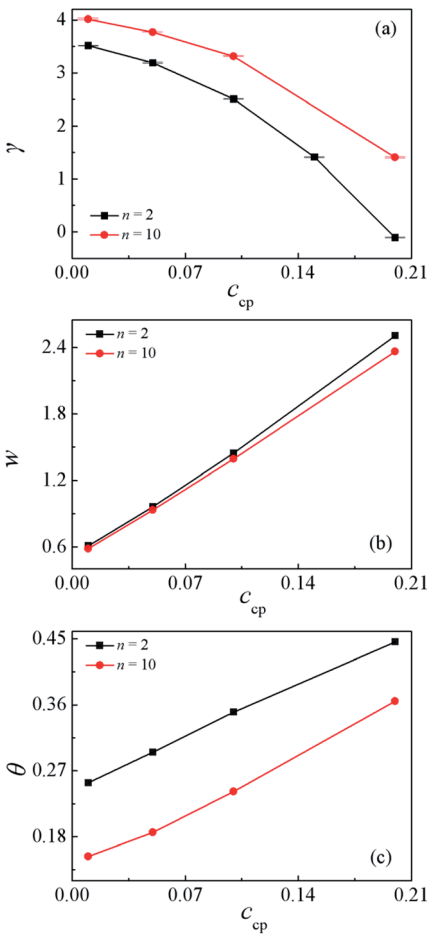

Fig. 4 Interfacial tension γ (a), interfacial width w (b), and orientation parameter Θ of the S_5M_5 diblock copolymer (c) as a function of the concentration of the S_5M_5 chains c_{cp} with $n = 2$ and $n = 10$.

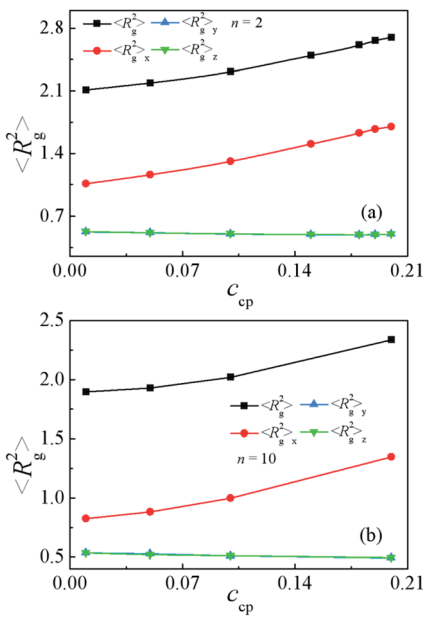

Fig. 5 Mean-square radii of gyration $\langle R_g^2 \rangle$ and the three principal components $\langle R_g^2 \rangle_x$, $\langle R_g^2 \rangle_y$, $\langle R_g^2 \rangle_z$ as a function of the S_5M_5 chain concentration c_{cp} with (a) $n = 2$ and (b) $n = 10$.

3.3 Effects of increasing the S_n and M_n homopolymers chain length n

In this section, the effect of increasing the S_n and M_n homopolymers chain length n on the interfacial properties of $S_n/S_5M_5/M_n$ ternary mixtures is discussed. Here, we vary the chain length of PS and PMMA homopolymers from $n = 2$ to 60 with $c_{cp} = 0.2$.

Fig. 6 shows the density distribution of beads S + M of the S_5M_5 diblock copolymer with different chain lengths n. We found that the density of S + M beads of the S_5M_5 copolymer at the center of the interface increases with the S_n and M_n homopolymers chain length increases from $n = 2$ to $n = 20$. However, as the chain length of the PS and PMMA homopolymers n increases from 20 to 60, the density of S + M beads of the S_5M_5 chains at the center of the interfaces remains almost unchanged.

Fig. 7(a) and (b) show the γ and w for the mixtures as a function of n, respectively. The obtained γ rapidly increases and the w decreases with increasing the $n = 2$ to 20, whereas both the γ and w almost remain unchanged when n increases from 20 to 60. These results show that $S_n/S_5M_5/M_n$ ternary mixtures composed of shorter S_n and M_n homopolymers exhibit lower interfacial tension γ. It is also revealed that the S_5M_5 diblock copolymers show better performance in lowering the γ for the mixtures with shorter S_n and M_n homopolymers. This is because that the shorter S_n and M_n homopolymers can cause a decayed correlation between the immiscible S_n and M_n homopolymers Fig. S3 in the ESI,† which results in a wider interfacial width w and a smaller interfacial tension γ.

Fig. 7(c) and 8 depict the dependence of the Θ and dimension of the S_5M_5 chains on the S_n and M_n homopolymer chain length n. It is found that the Θ, $\langle R_g^2\rangle$, $\langle R_g^2\rangle_x$, $\langle R_{ee}^2\rangle$ and $\langle R_{ee}^2\rangle_x$ decrease significantly with the increase of the S_n and M_n chain length from $n = 2$ to 20, while as the S_n and M_n chain length n further increases from 20 to 60, the Θ, $\langle R_g^2\rangle$, $\langle R_g^2\rangle_x$, $\langle R_{ee}^2\rangle$ and $\langle R_{ee}^2\rangle_x$ remain almost unchanged. Fig. 8(a) and (b) also show that as the n increases, the y and z components of the $\langle R_g^2\rangle$ and the $\langle R_{ee}^2\rangle$ always remain almost unchanged. These results can be interpreted as follows: when the chain length of the S_n and M_n homopolymers is very short $n = 2$, the S_5M_5 diblock copolymer at the interface resembles a "wet brush" (the homopolymers can penetrate the copolymer blocks layer),[48,49] and the S_5M_5 diblock copolymers are swollen by the short homopolymer

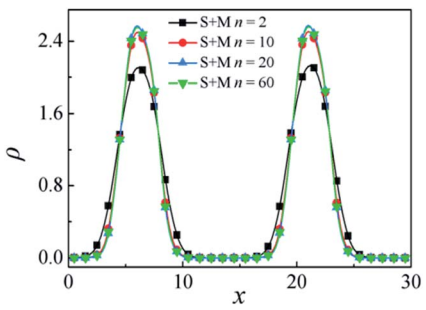

Fig. 6 Density profiles of beads S + M in the x-direction as a function of the PS and PMMA chain length n in mixture systems of S_5M_5.

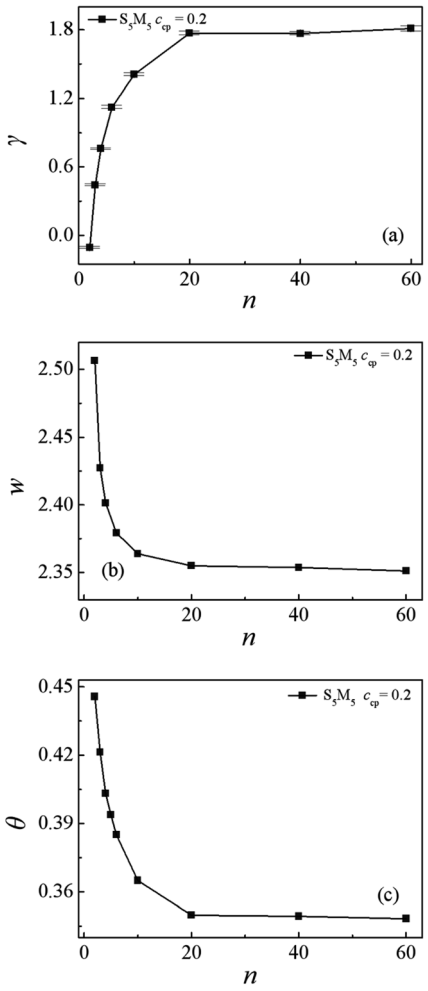

Fig. 7 (a) Interfacial tension γ, (b) interfacial thickness w, and (c) orientation parameter Θ of the S_5M_5 copolymers as a function of the PS and PMMA homopolymer chain length n in mixture systems of S_5M_5.

chain length. Thus, the S_5M_5 diblock copolymers are more stretched, accompanied by the larger Θ, the broader density distribution of the diblock copolymer, the wider interfacial width, and the smaller interfacial tension γ. When the $n \geq 20$, which are longer than the chain length of the S_5M_5 diblock copolymers 10, the homopolymers are expelled from the "dry brush",[48,49] *i.e.*, the S_n and M_n can't penetrate the S_5M_5 copolymers layer, therefore the density distribution of the S_5M_5 copolymers, the interfacial tension, and the configuration of the S_5M_5 copolymers remain unchanged as n further increases from 20 to 60.

We find that the interfacial properties of the $S_n/S_mM_m/M_n$ mixtures are strongly related to the S_n and M_n chain length n. And the study of Qian *et al.*[28] indicates that the interfacial tension of the A/AB/B ternary mixtures increases with the increasing of AB diblock copolymer chain length. However, the influence of simultaneously increasing S_mM_m, S_n, M_n chain lengths on the interfacial properties remains unclear. Therefore, in the next part, we investigate the effects of simultaneously increasing the S_mM_m, S_n, M_n chain length on the

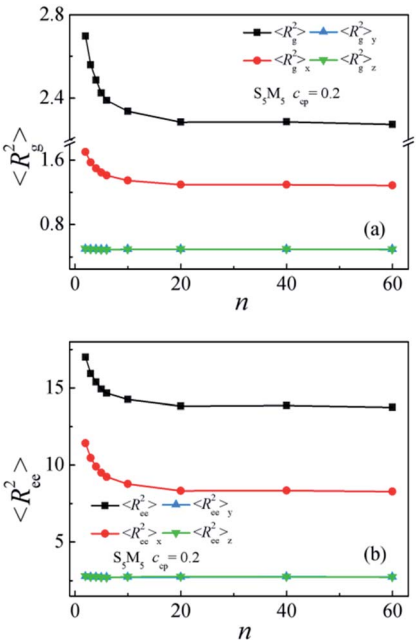

Fig. 8 (a) Mean-square radii of gyration $\langle R_g^2 \rangle$ and the three principal components $\langle R_g^2 \rangle_x$, $\langle R_g^2 \rangle_y$, $\langle R_g^2 \rangle_z$, (b) mean-square end-to-end distance $\langle R_{ee}^2 \rangle$ and the three principal components $\langle R_{ee}^2 \rangle_x$, $\langle R_{ee}^2 \rangle_y$, $\langle R_{ee}^2 \rangle_z$ as a function of n (n = 2, 3, 4, 5, 6, 10, 20, 40, 60).

interfacial properties with the chain length ratio of the S_mM_m and S_n, M_n fixed as $m = n$.

3.4 Effects of increasing the chain length of mixtures with $m = n$

The number of S and M beads for the copolymer and homopolymer used in this part are shown in Table 1.

Fig. 9 depicts the density profiles of the S_mM_m copolymer with different chain lengths with $m = n$ at a fixed S_mM_m chain concentration of $c_{cp} = 0.2$, which illustrates that the density of beads S + M of the S_mM_m diblock copolymer at the interfaces decreases with increasing $m = n$. According to Fig. 6, the density of beads S + M of the S_mM_m at the interfaces increases with increasing the n. Hence, we inferred that the decrease of the density of beads S + M of the S_mM_m chain at the center of the interfaces is mainly related to the increase of the S_mM_m chain length.[28]

Fig. 10(a) shows the dependence of the γ on the chain length $m = n$. Apparently, the obtained interfacial tension γ rapidly

Table 1 The number of S and M beads for S_mM_m diblock copolymer and S_n, M_n homopolymers

	$m = n$	
System	m	n
1	5	5
2	6	6
3	7	7
4	8	8

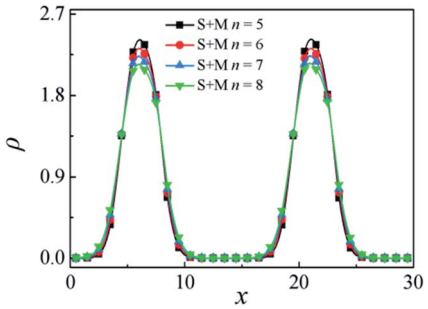

Fig. 9 Density profiles of beads S + M of the diblock copolymers in the x-direction as a function of the n with $m = n$.

increases with the increase of $m = n$. This result is in agreement with the findings of increasing the chain length of diblock copolymers,[28] which can be interpreted as follows: as the chain length $m = n$ increases, the $\langle R_g^2 \rangle_x$ increases, as shown in Fig S4.† It means that the copolymer chains with longer chain length penetrate more deeply into the homopolymer phase.

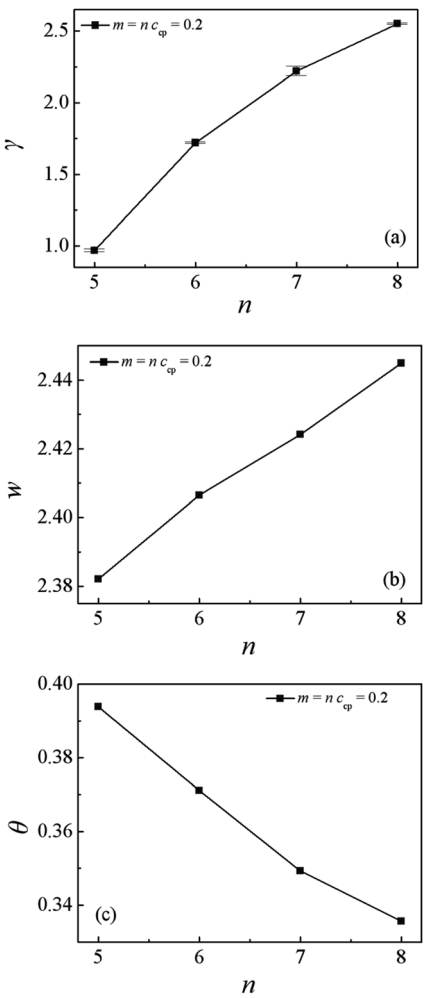

Fig. 10 (a) Interfacial tension γ, (b) interfacial width w, and (c) orientation parameter of the S_mM_m chain as a function of $m = n$ ($m = n$ = 5, 6, 7, 8).

Thus the number of the copolymers at the center of the interfaces decreases, and the interfacial tension increases.[28] Fig. 10(b) shows the relationship of the interfacial width w with the different chain lengths of $m = n$. We find that the interfacial width w increases with increasing the diblock copolymer and homopolymer chain length $m = n$. According to the result in the previous part, we know that as the chain length of the S_n and M_n homopolymers increase from 2 to 10 at a fixed chain length of diblock copolymers, the interfacial width w decreases. It means that the increase of the interfacial width w is also mainly related to the increase of the chain length of diblock copolymers. Fig. 10(c) shows the orientation parameter Θ of the diblock copolymers at the different chain lengths of $m = n$. We found that as $m = n$ increases from 5 to 8, the orientation parameter Θ decreases, which is in contrast to the result of increasing diblock copolymer chain length with the homopolymer chain length n fixed.[28] Therefore, we deduce that the decayed stretching of the diblock copolymer is mainly dependent on increasing the S_n and M_n homopolymer chain length n.

4. Conclusions

In this paper, we conducted dissipative particle dynamics (DPD) simulations to study the three effects on the interfacial properties, including: the increase of the S_mM_m diblock copolymer concentration; the chain lengths of homopolymers S_n and M_n (the chain length of the S_mM_m copolymer is fixed as 10); and the simultaneous change of chain lengths of S_mM_m, S_n, and M_n with $m = n$.

Our simulation results show that when the concentration of the S_mM_m diblock copolymers $c_{cp} \leq 0.2$, the S_mM_m diblock copolymers are segregated at the flat interfaces, and the S and M beads of the S_mM_m chains segregate into the homopolymers bulk S_n and M_n phases, respectively. As the S_mM_m diblock copolymer concentration c_{cp} increases from 0.01 to 0.2, the density of S + M beads of the S_mM_m copolymer at the center of the interfaces increases, which results in the decayed correlations between S_n and M_n homopolymers, hence the interfacial tension decreases.

We then explore the interfacial properties of the $S_n/S_mM_m/M_n$ mixtures with different chain lengths. (1) For the case of increasing the S_n and M_n homopolymers chain length n, when the $n \leq 10$, the S_5M_5 diblock copolymers at the interface are swollen by the shorter homopolymers and resemble a "wet brush". As the homopolymer chain length is shorter with $n = 2$, the S_5M_5 diblock copolymers are more stretched, accompanied by the larger Θ, the broader density distribution of the diblock copolymer, the wider interfacial width w, and the smaller interfacial tension γ. When $n > 10$, the homopolymers are expelled from the "dry brush". Furthermore, as n further increases from 20 to 60, the density distribution of the S_5M_5 copolymers, the interfacial tension, and the configuration of the S_5M_5 copolymers remain unchanged. (2) For the case of simultaneously increasing chain lengths of S_mM_m, S_n, M_n with $m = n$, the deep of copolymer penetrate into the homopolymer phase increases with increasing $m = n$, which results in the weakened interactions between diblock copolymers and the increased interfacial tension, meanwhile, the orientation parameter Θ decreases, which is in contrast to the result of increasing diblock copolymer chain length with n fixed. It means that the decrease of the Θ is mainly related to the increase of the homopolymer chain length n.

Our simulation results indicate that the interfacial properties of $S_n/S_mM_m/M_n$ mixtures are strongly correlated to the concentration of the S_mM_m chains and the chain lengths of S_mM_m, S_n, M_n, which raises important considerations concerning the use of the diblock copolymer as compatibilizers in the immiscible mixture systems.

Conflicts of interest

There are no conflicts to declare.

Acknowledgements

This work is financially supported by the Basic Scientific Research Project of Hebei Provincial Department of Education (grant JQN2020021). We are grateful for the essential supports of Hebei Key Laboratory of Data Science and Application.

References

1 L. Sperling, in *Recent Advances in Polymer Blocks, Grafts, and Blends*, Plenum Press, 1974.
2 D. R. Paul and J. W. Barlow, *J. Macromol. Sci., Polym. Rev.*, 1980, **18**, 109.
3 I. C. Sanchez, *Annu. Rev. Mater. Res.*, 1983, **13**, 387–412.
4 S. H. Wu, *Polym. Eng. Sci.*, 1987, **27**, 335–343.
5 K. Binder, M. Muller, F. Schmid and A. Werner, *Phys. A*, 1998, **249**, 293–300.
6 N. Tan, S. K. Tai and R. M. Briber, *Polymer*, 1996, **37**, 3509–3519.
7 H. Liang, B. D. Favis, Y. S. Yu and A. Eisenberg, *Macromolecules*, 1999, **32**, 1637–1642.
8 T. P. Russell, A. Menelle, W. A. Hamilton and G. S. Smith, *Macromolecules*, 1991, **24**, 5721–5726.
9 P. F. Green and T. P. Russell, *Macromolecules*, 1991, **24**, 2931–2935.
10 T. P. Russell, S. H. Anastasiadis, A. Menelle, G. P. Felcher and S. K. Satija, *Macromolecules*, 1991, **24**, 1575–1582.
11 S. H. Anastasiadis, T. P. Russell, S. K. Satija and C. F. Majkrzak, *J. Chem. Phys.*, 1990, **92**, 5677–5691.
12 S. H. Anastasiadis, T. P. Russell, S. K. Satija and C. F. Majkrzak, *Phys. Rev. Lett.*, 1989, **62**, 1852–1855.
13 G. L. Liu, M. P. Stoykovich, S. X. Ji, K. O. Stuen, G. S. W. Craig and P. F. Nealey, *Macromolecules*, 2009, **42**, 3063–3072.
14 K. Chang, C. W. Macosko and D. C. Morse, *Macromolecules*, 2015, **48**, 8154–8168.
15 L. B. Fischel and D. N. Theodorou, *J. Chem. Soc., Faraday Trans.*, 1995, **91**, 2381–2402.
16 A. C. Balazs, C. P. Siemasko and C. W. Lantman, *J. Chem. Phys.*, 1991, **94**, 1653–1663.
17 Y. M. Wang, Y. Li and W. L. Mattice, *J. Chem. Phys.*, 1993, **99**, 4068–4075.

18 F. Schmid and M. Müller, *Macromolecules*, 1995, **28**, 8639–8645.
19 M. Müller and M. Schick, *J. Chem. Phys.*, 1996, **105**, 8885–8901.
20 A. Werner, F. Schmid, K. Binder and M. Müller, *Macromolecules*, 1996, **29**, 8241–8248.
21 T. Uneyama and M. Doi, *Macromolecules*, 2005, **38**, 196–205.
22 B. Vorselaars, R. K. W. Spencer and M. W. Matsen, *Phys. Rev. Lett.*, 2020, **125**, 117801.
23 R. K. W. Spencer and M. W. Matsen, *J. Chem. Phys.*, 2018, **148**, 204907.
24 D. Duchs, V. Ganesan, G. H. Fredrickson and F. Schmind, *Macromolecules*, 2003, **36**, 9237–9248.
25 F. S. Bates, W. W. Maurer, P. M. Lipic, M. A. Hillmyer, T. P. Lodge, K. Almdal, K. Mortensen and G. H. Fredrickson, *Phys. Rev. Lett.*, 1997, **79**, 849–852.
26 D. Broseta and G. H. Fredrickson, *J. Chem. Phys.*, 2018, **148**, 204907.
27 K. Uchida, K. Mita, S. Yamamoto and K. Tanaka, *ACS Macro Lett.*, 2020, **9**, 1576–1581.
28 H. J. Qian, Z. Y. Lu, L. J. Chen, Z. S. Li and C. C. Sun, *J. Chem. Phys.*, 2005, **122**, 187907.
29 H. Guo and M. Cruz, *J. Chem. Phys.*, 2005, **123**, 753.
30 T. Lemos, C. Abreu and J. C. Pinto, *Macromol. Theory Simul.*, 2020, **29**, 1900042.
31 A. D. Goodson, G. Liu, M. S. Rick, A. W. Raymond, M. F. Uddin, H. S. Ashbaugh and J. Albert, *J. Polym. Sci., Part B: Polym. Phys.*, 2019, **57**, 794–803.
32 R. D. Groot and P. B. Warren, *J. Chem. Phys.*, 1997, **107**, 4423–4435.
33 X. H. Liu, Z. Q. Bai, K. D. Yang, J. Y. Su and H. X. Guo, *Sci. China: Chem.*, 2013, **56**, 1710–1721.
34 J. J. Wang, Z. Z. Li, X. P. Gu, L. F. Feng, C. L. Zhang and G. H. Hu, *Polymer*, 2012, **53**, 4448–4454.
35 S. H. Anastasiadis, I. Gancarz and J. T. Koberstein, *Macromolecules*, 1988, **21**, 2980–2987.
36 C. Zhou, S. K. Luo, Y. Sun, Y. Zhou and W. Qian, *J. Appl. Polym. Sci.*, 2016, **133**, 44098.
37 F. Paiva, A. Boromand, J. Maia, A. Secchi, V. Calado and S. Khani, *J. Chem. Phys.*, 2019, **151**, 114907.
38 Y. Zhou, X. P. Long and Q. X. Zeng, *Polymer*, 2011, **52**, 6110–6116.
39 Z. L. Luo and J. W. Jiang, *Polymer*, 2010, **51**, 291–299.
40 D. M. Liu, X. Z. Duan, T. F. Shi, F. Jiang and H. Z. Zhang, *Chem. J. Chin. Univ.*, 2015, **36**, 2532–2539.
41 D. M. Liu, L. J. Dai, X. Z. Duan, T. F. Shi and H. Z. Zhang, *Chem. J. Chin. Univ.*, 2015, **36**, 1752–1758.
42 D. M. Liu, K. Gong, Y. Lin, T. Liu and X. Duan, *Polymers*, 2021, **13**, 1516.
43 D. M. Liu, K. Gong, Y. Lin, H. F. Bo, T. Liu and X. Z. Duan, *Polymers*, 2021, **13**, 2866.
44 D. M. Liu, M. Y. Yang, D. P. Wang, X. Y. Jing, Y. Lin, L. Feng and X. Z. Duan, *Polymers*, 2021, **13**, 2333.
45 P. Espanol and P. B. Warren, *J. Chem. Phys.*, 2017, **146**, 150901.
46 F. Goodarzi and S. Zendehboudi, *Ind. Eng. Chem. Res.*, 2019, **58**, 8817–8834.
47 A. G. Alexey, V. K. Yaroslav and V. C. Alexander, *J. Chem. Phys.*, 2013, **139**, 224901.
48 P. K. Janert and M. Schick, *Macromolecules*, 1997, **30**, 137–144.
49 I. Fortelny and J. Juza, *Polymer*, 2018, **150**, 380–390.